An integrated multi-objective optimization and multi-criteria decision-making model for optimal planning of workplace charging stations.

ERDOGAN, N., PAMUCAR, D., KUCUKSARI, S. and DEVECI, M.

2021

An integrated multi-objective optimization and multi-criteria decision-making model for optimal planning of workplace charging stations*

Nuh Erdogan[a,*], Dragan Pamucar[b], Sadik Kucuksari[c] and Muhammet Deveci[d]

[a]School of Engineering, Robert Gordon University, Aberdeen AB10 7GJ, UK
[b]Department of Logistics, Military Academy, University of Defence in Belgrade, 11000 Belgrade, Serbia
[c]Department of Technology, University of Northern Iowa, Cedar Falls, IA, 50614, USA
[d]School of Computer Science, University of Nottingham, Nottingham, NG8 1BB, UK

ARTICLE INFO

Keywords:
Electric vehicles
EVSE
multi-objective optimization
multi-criteria decision making
workplace charging

ABSTRACT

This study addresses the optimal planning of electric vehicle charging infrastructure at workplaces. As the optimal planning for a given workplace can involve various criteria that comprise conflicting single objectives, this study proposes a new integrated multi-objective optimization and multi-criteria decision-making (MCDM) model for determining the most suitable electric vehicle supply equipment (EVSE) configuration. This approach combines the advantage of multi-objective optimization, which yields Pareto solutions, with an improved MCDM model. The latter is used to evaluate the Pareto frontier to find the best performing solution by enabling the station owners to use linguistic variables for weighting the decision-making variables. The conventional weighted aggregated sum product assessment method is improved by introducing the Dombi Bonferroni functions in the proposed model making it more flexible as compared to its counterparts. In the final step, the selected solutions are ranked by reapplying the MCDM model. A case study is performed based on collected charging data from a workplace. To validate the proposed model, a comparison against four alternative MCDM models is performed. It is demonstrated that the proposed model yields very close ranking order as the alternative approaches. Among five EVSE options, DC fast charging is found to be the best while AC Level-2 EVSE (19.2/22kW) is found to be the least attractive option. Sensitivity analysis shows the robustness of the ranking results in response to changing weightings of the model coefficients.

1. Introduction

Global deployment of electric vehicle (EV) charging infrastructure is gradually increasing to respond to ever-increasing EV market share worldwide. Governments have introduced a range of policies and incentives to promote further deployment of the charging infrastructure. Accordingly, the number of global EV charging units continues to rise reaching about 7.3 million chargers worldwide in 2020 [1]. Workplace charging is the second most preferred charging modality [2]. Enabling more charging units at workplaces provides benefits in several ways. First, it can mitigate charger access anxiety that will increase the electric driving range for EVs [3]. This is essential to boost up EV adoption since the lack of charging infrastructure is still one of the most commonly reported barriers to the EV transition [1]. Second, it will help companies transition their vehicles towards an electric fleet [4]. Moreover, workplaces can play a strategic charging infrastructure role

*This work forms part of the E-fleet project which is funded by Sustainable Energy Authority of Ireland (SEAI) under the grant agreement number RDD527.

*Corresponding author
n.erdogan@rgu.ac.uk (N. Erdogan); dpamucar@gmail.com (D. Pamucar); sadik.kucuksari@uni.edu (S. Kucuksari); muhammet.deveci@nottingham.ac.uk (M. Deveci)

to shift EV charging loads from peak demand times to daytime charging for employees' vehicles or night charging for fleet cars. As such, workplace charging can help integrate variable renewable generation [5]. EV charging infrastructure at workplaces should, therefore, be stimulated.

Planning and managing a workplace charging station requires an optimal design that needs to address the issues from the perspectives of the station owner, EV users, and the grid [6]. It should provide a cost-effective solution for both EV users and the station owner without compromising an efficient use of the grid assets [7]. Optimal charging station sizing and placing have, therefore, been an ongoing research focus for many researchers. Single-objective optimization approach has been widely applied to formulate the planning problem in most of these studies [2]. In this approach, several different objectives are lumped into a single objective function. Then, deterministic models based on linear [8] and nonlinear integer programming [9] or meta-heuristic models [10] are typically used to find the best solution. In [2], the sum of three cost elements associated with electric vehicle supply equipment (EVSEs) is minimized to find the least lifetime cost of a workplace charging station. In [8], the use of various non-residential EVSEs is maximized for increased number of EVs served. Li et al. in [11] analyzes the techno-economic feasibility of various configurations of a given workplace charging station. While the overall objective of these research is to maximize either EV user or the station owner's profit, technical aspects associated with charging station deployment such as network losses and the grid impact are not considered. Further work included the effect of power grid constraints such as network losses and voltage profiles in optimizing the siting and sizing of non-residential charging stations [12]. The objective is set to reduce losses and improve the voltage profile in the distribution system in [12]. Luo et al. in [13] lumped the costs of network reinforcement and losses in a single cost function. While these single-objective optimization models provide an optimal charging infrastructure configuration through cost minimization, the solution is sought for only a specific criterion or metric that corresponds to minimizing a single objective function aggregating all different objectives into one. However, the planning problem for a given workplace environment can involve several conflicting objectives when all aspects of a charging station is considered. Some of these objectives can be compromised in finding the optimal solution if considered independently as single-objective optimizations. For instance, optimising charging powers for EVs that minimizes only the energy charge considered as the single objective can increase the peak demand. This might result in higher demand charges for industrial and commercial customers [14]. Therefore, each aspect for a given workplace should be considered in finding the optimality that results in multiple non-unique sets of solutions. The final subjective decision can then be made from the non-dominated solutions, i.e., Pareto optimal set based on the decision maker's priority [15]. In this respect, the multi-objective optimisation method can define a Pareto optimal set that provides a suitable compromise among all objectives without degrading any of them.

The multi-objective optimization (MOO) approach has been mainly applied to location optimization of public charging infrastructure [16]. Considering both the grid and EV user related objectives, the electric vehicle grid integration is optimized [17]. These studies apply various evolutionary algorithms such as multi-objective evolutionary algorithms based on decomposition, non-dominated sorting genetic algorithms, multi-objective grey wolf optimiser for finding Pareto solutions [18]. Herein, the meta-heuristic solutions can be very time inefficient. For instance, an ant colony optimization-based approach requires around 127s to find the best route for an EV in [19] that can be prohibitive to be implemented in real-time. Pareto ranking selection should therefore be practical for real-time applications. Furthermore, premature convergence to a suboptimal point may result in adverse configuration. In [20], the weighted sum approach is adopted to assign a chosen weight of the user's priority to each objective function. However, this approach converts the multi-objective problem into a single scalar objective function. Only single solution among the Pareto solutions are found that does not yield the global optimum point. Multi-criteria decision making (MCDM) methods such as technique for order of preference by similarity to ideal solution (TOPSIS) have been recently applied to the siting problem of public electric vehicle charging stations. Shi & Lee in [21], TOPSIS method is employed to

select a final satisfied solution among the Pareto set. It is shown that the multi-objective optimisation model provides better balanced solution as compared to the single objective optimisation. Liu et al. in [22], two MCDM methods, namely, decision-making trial and evaluation laboratory and multi-objective optimization by ratio analysis plus full multiplicative form are integrated to manage the decision makers' uncertain and diverse linguistic assessments in optimizing the location of public charging stations. It has been shown that MCDM methods can provide effective rankings under an uncertain linguistic context when involving many conflicting criteria. While the above literature indicates that charging station site selection is often researched based on various objectives, optimal configuration of charging stations is largely unexplored. Furthermore, to the best of authors' knowledge, the MCDM approach has not been applied to find the best performing Pareto solution whereas they have been typically used in ranking charging station sites. Particularly, the MCDM methods in EV applications have been employed based on the assumption that decision-making variables are independent [22]. However, decision-making variables are expected to be interrelated when all aspects for a workplace charging station are considered. Therefore, further work on MCDM methods is needed in terms of improving flexibility and respect for the mutual influence among the attributes of decision. That means that the method respects the mutual influence between the attributes in the initial decision matrix.

With the motivations stated above, this study proposes an improved MCDM model to select the best performing EVSE configuration among optimal options based on the designer's perspective (e.g., the workplace charging station owner). The optimal EVSE configurations are first obtained from a developed MOO model. In the proposed MCDM model, the weighted aggregated sum product assessment (WASPAS) method was extended using Dombi Bonferroni functions. The latter are used to determine weighted sequences and form an aggregation function based on which the optimal alternative is selected. To the best of the authors' knowledge, no research considers the fusion of information using Dombi Bonferroni functions in the WASPAS methodology to date. Unlike the current MCDM approaches such as WASPAS, combined compromise solution (CoCoSo) method, Multi-Attributive Border Approximation Area Comparison (MABAC), and MultiAtributive Ideal-Real Comparative Analysis (MAIRCA) that utilize linear functions based on weight arithmetic averaging, nonlinear aggregation functions are used based on the implementation of Dombi norms in the Bonferroni functions. That makes it a more flexible decision-making method as compared to its counterparts. The main feature of the presented model is the way of determining the weight coefficients of decision-making variables for defining the relationship among the variables that is based on the application of the logarithmic additive function and Dombi norms. Furthermore, the MCDM methods in the current literature such as WASPAS, CoCoSo, MABAC, and MAIRCA require the application of other objective or subjective methodologies to determine the weighting coefficients of the criteria [23, 24, 25]. The main advantages of the improved WASPAS model can be highlighted as follow: *(i)* enabling flexible decision-making and taking into account the interaction between decision attributes, *(ii)* considering the connection between the attributes and eliminating the impact of extreme/inconsistent data, *(iii)* possessing the flexibility that is expressed by the parameters μ_1, μ_2, and δ, *(iv)* allowing to control the robustness of the results by varying the parameters μ_1, μ_2, and δ and their influence on the final decision. In this respect, the Dombi Bonferroni WASPAS method provides a fully defined multi-criteria framework that enables the definition of criterion weights and the evaluation of alternatives. Overall, the main salient contributions of this study can be summarized as follows:

- A new methodology is proposed for selecting the best performing option for Pareto solutions. As such, this methodology enables individual expert evaluations in a multi-criteria decision-making framework to find an optimal electric vehicle supply equipment (EVSE) configuration at workplaces.
- A multi-objective optimization model for workplace charging stations is proposed that minimizes overall cost of a workplace charging station for its lifecycle including daily levelized infrastructure cost, energy, and demand charges.

- The conventional WASPAS model is improved by introducing Dombi Bonferroni functions making it more flexible as compared to its counterparts.

The rest of this paper is organized as follows. Section 2 presents the proposed methodology including the description of EVSE alternatives considered. The MOO model is presented in Section 3. Section 4 presents the Dombi Bonferroni WASPAS model along with detailing the decision-making variables considered. Experimental and comparison results, including a sensitivity analysis, are discussed in Section 5. Finally, Section 6 provides concluding remarks.

2. Methodology

2.1. Approach

The flowchart for the optimal planning of workplace charging station proposed is presented in Fig. 1. Here, the optimal solution is sought from a charging station operator perspective, since facility managers at workplaces usually supervise the charging and billing procedure. In seeking the optimal charging infrastructure, the methodology is proposed to combine the advantages of MOO with those of MCDM approaches. As such, the MOO can optimize several conflicting objectives simultaneously that yield a set of optimal solutions (i,e., Pareto frontier) [22] while the MCDM provides formulation flexibility and easy calculation in evaluating the solutions from the multi-criteria perspectives considered, which in turn determines the best performing solution [15]. The model first relies on collected data from charging units that are used to extract a charging behavior. Then, an MOO model is developed in which various aspects of a charging station operator are considered with different objectives. The model is run for different EVSE configurations that are currently installed at workplaces. The Pareto frontier for each EVSE is evaluated by proposed Dombi Bonferroni WASPAS model enabling experts to use linguistic variables for weighting evaluation criteria. As such, the best performing optimal solution for each candidate configuration is found. Finally, the selected solutions are ranked by reapplying the Dombi Bonferroni WASPAS model. The validation of the ranking results obtained are made by comparing with those of other four MCDM methods, i.e., WASPAS, MABAC, MAIRCA, and CoCoSo.

2.2. Description of alternatives

A charging station consists of an EVSE to deliver electricity to an EV through a standardized connector and a dedicated socket outlet. It can be either an AC inlet incorporating protection, control, and communication devices, or an AC-DC converter with communication and control functions installed in. There are currently two standards, namely, the Standard J1772 [26] and the Standard IEC 61851 [27] that define the requirements, allowable charging rates, and the handshake protocol that EVSE and EV must follow in North America and Europe, respectively. Both standards classify EVSEs into three categories as either *levels* in J1772 or *modes* in IEC 61851 based on power rates at which EV's battery is charged. The first EVSE type is AC *Level-1* or *Mode-2* providing AC charging power to the vehicle from single phase plug through a dedicated charging cable and socket outlet such as Mennekes. It does not require any additional infrastructure. However, the maximum charging power can be up to 1.9/3.68 kW (max 16 A) depending on supply voltage that provides a low-speed charging. Therefore, this EVSE type is typically used in residential areas with long parking times. The second EVSE is AC *Level-2* or *Mode-3* that offers smart charging through a dedicated socket outlet in which the charging process can be monitored, controlled, and managed [28]. It can be supplied from either single phase (L2-1P) or three phase (L2-3P) that allows medium-speed charging up to 7.36 kW (max 32 A) and fast charging 19.2/22 kW (240V-80A/400V-32A), respectively. The *Mode 3* in Europe has also rapid charging capability of up to 43 kW (max 63A). This EVSE is typically installed at workplaces with moderate parking dwell times. The third EVSE type is on the other hand DC fast charger (DCFC) or *Mode-4* that enables rapid charging at a range of high power levels from 50 kW to 350 kW. The

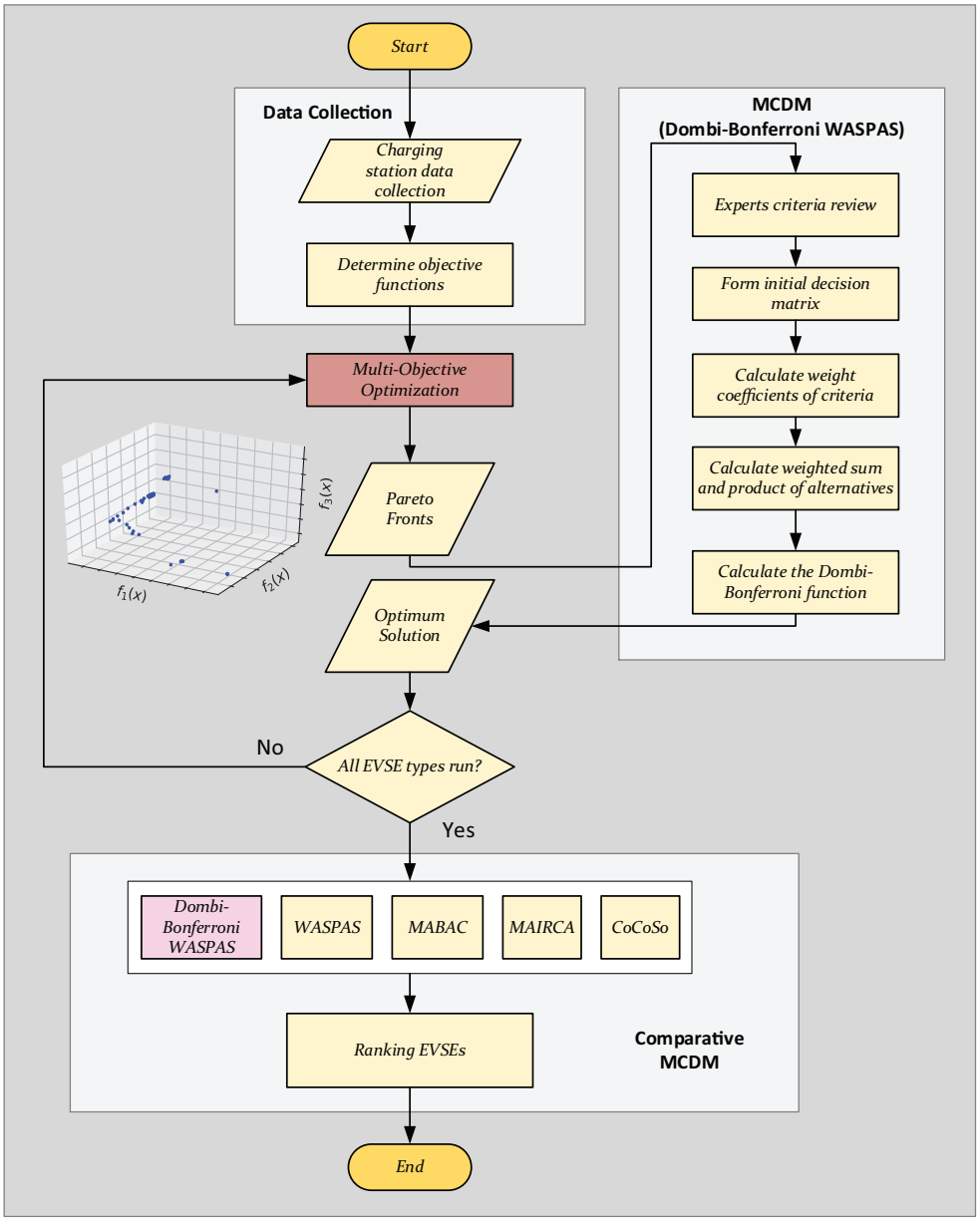

Figure 1: Flowchart of proposed integrated approach.

charging rate can be limited depending on the vehicle's acceptance rate. Unlike AC EVSEs in which the charger is built into the vehicle, DCFC includes a bidirectional high-power AC-DC converter that provides DC electricity directly to the vehicle's battery. DCFC requires specific connectors such as either Combo-2, CHAdeMO or GB/T [29]. Similar to L2 types, DCFC units are installed at workplaces, public car parks, and on-street parking. Both L2 and DCFC types have multi-port options (typically 2 ports) that enable EVs to charge simultaneously by sharing the supply across the ports. L2 and DCFC installations at workplaces mostly require electrical upgrades and are subject to site factors including visibility and aesthetics that increase the installation cost significantly. Moreover, their commercial installations may result in higher electricity costs by increasing the facility's peak electricity demand. This study considers available five

different EVSE types to be installed at workplaces. These are L2-1P, L2-3P, DCFC including multi-port L2-3P (L2 MP) and multi-port DCFC (DCFC MP).

3. Multi-objective optimization cost model for workplace charging stations

MOO methods are commonly used to solve a variety of design problems with multi objective functions to be satisfied at the same time. These multiple design objectives enforce contradicting requirements on the technical and economic performances of a system [30]. MOO provides superiority over single-objective optimization by providing concurrently achieved trade-off between the multiple single objective functions [15]. This results in a set of solutions, called Pareto frontier, in which the optimal solution for one objective may not be the optimal for other objectives [31]. Final selection among Pareto frontier can be made based on the decision maker's preferences [32].

Several cost objectives can be defined from the workplace EV charging station owner perspective. An EVSE cost function can be classified as capital and operational expenditures. The major capital expenditure (CAPEX) is EVSE unit cost ($/unit) that varies from type and size. The operational expenditure (OPEX) includes two cost elements. The first element is the energy charge that represents daily electricity consumption cost to charge all EVs in a workplace charging station. It can be sensitive to smart charging strategies while charging scheduling policies can affect greatly the energy charges under utility time-of-use (TOU) tariffs ($/kWh) [33]. The second is demand charge that corresponds to the contribution of charging loads to peak demand of facility. Unlike the residential customers, industrial and commercial customers are subject to demand charges as an additional cost for their monthly peak power consumption measured as the average of 15 min time intervals [2]. This becomes a major concern in EV adaption at workplaces since EV charging can increase the peak demand significantly [34]. As a result, monthly bill may be higher due to the high demand charge even though the energy charge is minimized.

Finding the trade-off between these cost functions as objectives requires a MOO model. The model is presented in which the CAPEX and OPEX are to be optimized together. The model includes three cost functions. C_{op} in (1) is the daily operational cost referring to cost of daily total electricity consumption to charge all EVs. Typical TOU rate with varying energy cost is considered as a price vector of $F(t)$ taken from [35]. To satisfy EV users requirements, the operational cost function is subject to the constraints given in (2) through (5) . The constraint (2) make sure that the required charging energy of the i^{th} EV, $E_{required,i}$, is satisfied within the vehicle's arrival, $t_{arr,i}$, and departure, $t_{dept,i}$, times. The constraint (3) states that the charging power of the i^{th} EV, $P_{ch,i}$, can be between zero and minimum of rated powers of EVSE (P_j^{rated}) and EV's on-board charger (P_i^{rated}). η_j and η_i denotes efficiencies of EVSE and on-board charger of i^{th} EV, respectively. Constraint (4) imposes that the charging process happens within the arrival and departure times. Constraint (5) states that the required charging time, $t_{req,i}$ cannot be longer than the plugged in time. Herein, $N=\{1,2,...n\}$ is set of EVs, T is the number of time slots of 1 min each, $S=\{1,2,...s\}$ is set of EVSE units, $J=\{1,2,3,4,5\}$ is set of charging levels of the EVSE types considered. $\{1,2,3,4,5\}$ denotes L2-1P, L2-3P, L2 MP, DCFC and DCFC MP charging units, respectively. P_J^{rated} and η_J are the rated power and the efficiency of DCFC EVSE unit, respectively.

$$C_{op} = \sum_{s_j=1}^{S_j} \sum_{i=1}^{n} \sum_{t=1}^{T} \Big(F(t) \times (P_{ch,i,s_j}(t) \cdot \frac{\Delta t}{60}) \Big), \tag{1}$$

$$\text{subject to} \quad \sum_{t=1}^{T} P_{ch,i}(t) \cdot \eta_i \cdot \frac{\Delta t}{60} = E_{required,i}, \qquad \forall t \in [t_{arr,i}, t_{dept,i}], i = 1, ..., n \tag{2}$$

$$\begin{cases} 0 \le P_{ch,i}(t) \le min\Big(\eta_i P_i^{rated}, \eta_j P_j^{rated}\Big), \forall J \in \{1,2,3\} \\ 0 \le P_{ch,i}(t) \le \eta_J \cdot P_J^{rated}, \forall J \in \{4,5\} \end{cases} \quad \forall t \in [t_{arr,i}, t_{dept,i}], i = 1, ..., n \tag{3}$$

$$P_{ch,i}(t) = 0, \qquad \forall t \notin [t_{arr,i}, t_{dept,i}], i = 1, ..., n \tag{4}$$

$$t_{req,i} \le (t_{dept,i} - t_{arr,i}), \qquad i = 1, ..., n. \tag{5}$$

The second cost function is the demand charge , C_{dc}, as given in (6). It is the product of a demand charge rate, C_{drate} and the peak power of daily aggregated load profile in 15 min interval. The daily aggregated load profile is the sum of base demand of the workplace, P_{base}, and total charging loads, $\sum P_{ch,i,s_j}$. It is dynamically updated after each EV charging is scheduled. Demand charge with TOU tariff given in [35] is considered as the price information. The constraint in (7) guarantees that the maximum power of the workplace, P_{lim}, is limited to 500 kW since the rate is designed for customers with a demand up to 500 kW.

$$C_{dc} = C_{drate} \cdot \Big(max\Big(\sum_{k=1}^{96}\sum_{t=1}^{15} mean\Big(P_{base}((k-1)\cdot 15 + t) + \sum_{s_j=1}^{S_j}\sum_{i=1}^{n} P_{ch,i,s_j}((k-1)\cdot 15 + t)\Big)\Big)\Big), \tag{6}$$

$$\text{subject to} \sum_{t=1}^{T}\Big(P_{base}(t) + \sum_{s_j=1}^{s_j}\sum_{i=1}^{n} P_{ch,i,s_j}(t)\Big) \le P_{lim}, \qquad S_j = 1, ..., s_j, i = 1, ..., n. \tag{7}$$

The third cost function is the daily-levelized EVSE infrastructure cost, C_{EVSE}, as given in (8), that includes unit hardware, C_{unit}, installation, C_{ins}, and maintenance C_{main} costs [36]. While minimizing energy and demand charges, the EVSE cost may increase due to the need of higher number of units. Since the unit cost for EVSE is significant, the savings from the energy and demand charges may be suppressed. An annuity factor, AF, given in (9) is used to convert the infrastructure cost to a daily-levelized cost with a fixed interest rate of 5%. The costs of unit, installation, and maintenance are considered as lump sum of \$5,000, \$12,000, and \$50,000 for L2-1P, L2-3P, and DCFC, respectively taken from [37].

$$C_{\text{EVSE}} = AF \cdot s_j \cdot \Big(C_{unit} + C_{ins} + C_{maint}\Big). \tag{8}$$

$$AF = \Big(\frac{1}{WD} \cdot \frac{(1+r)^{LC} \cdot r}{(1+r)^{LC} - 1}\Big). \tag{9}$$

The three conflicting cost functions are optimized simultaneously using multi-objective optimization given in (10). Due to the contradictory nature of the cost functions, there is no single solution that minimizes each cost functions simultaneously, therefore, a set of Pareto optimum solutions exist [38]. The Pareto optimality can be achieved with a common method of weighted sum approach by forming a single objective function $\mathcal{F}$ in (11). It is a weighted linear combination of all the three cost functions [39]. The sum of weights in the aggregated function should be one (12). An increment of 0.1 is selected to evaluate the range of weights (ω_1, ω_3, and ω_3) in minimizing $\mathcal{F}$ that resulted in 66 possible cases and corresponding solutions as the Pareto optimality. Among these solutions, the optimum solution is decided based on the station owner's preferences using the proposed MCDM that enables station owner to evaluate various criteria, which is explained in the next section.

$$\min_{\substack{P_{ch,1}\cdots P_{ch,n} \\ S_j}} \Big[C_{op}(P_{ch,i}, S_j), \quad C_{dc}(P_{ch,i}, S_j), \quad C_{\text{EVSE}}(S_j)\Big]^T. \tag{10}$$

Table 1
The evaluation criteria.

Criteria Code	Criteria Name	Unit	Type
C_1	Peak demand	kW	Cost
C_2	Number of EVSE units	-	Cost / Benefit
C_3	Energy charge	Cents/kWh	Cost
C_4	Demand charge	Cents/kWh	Cost
C_5	EVSE cost	Cents/kWh	Cost
C_6	EVSE occupancy	%	Cost
C_7	Required charging time	min	Cost
C_8	Hosting capacity	%	Benefit
C_9	Lifetime of EVSE unit	years	Benefit
C_{10}	User flexibility	%	Benefit

$$\mathcal{F}(P_{ch,i}, S_j) = \Big(\omega_1 \cdot C_{op}(P_{ch,i}, S_j) + \omega_2 \cdot C_{dc}(P_{ch,i}, S_j) + \omega_3 \cdot C_{\text{EVSE}}(S_j)\Big), \tag{11}$$

with,

$$\omega_1 + \omega_2 + \omega_3 = 1, \quad \forall\, \omega \in [0, 1]. \tag{12}$$

To solve the optimisation problem (10), an interrupted smart charging strategy with the first-come, first-served scheduling policy is employed in the model. This algorithm minimizes the number of charging units that places EVs into a charging unit sequentially depending on their arrival time until an incoming EV cannot be fit in the current charging unit. Then, a new charging point is added and the incoming EV is placed in the new unit. The algorithm imposes an interrupted charging profile in which the EV is charged at discrete time slots that may be separated by idle slots [40]. The model is implemented in Matlab using the optimization toolbox as a linear programming [41]. Based on collected data from the field, the arrival and departure times and the required charging energy for EVs are assumed to be Gaussian. The arrival and departure times are a mean of 8:40 A.M. with a standard deviation of 1h 05, and a mean of 4:10 P.M. with a standard deviation of 2h 28, respectively. % SoC levels of EVs are a mean of 45% and a standard deviation of 18%. Simulations are run for a group of 100 EVs for 100 random cases that covers different mobility scenarios.

4. Multi-criteria decision-making model for the Pareto solutions

4.1. Description of decision-making variables

This study specifies key variables in evaluating the optimal configuration of a workplace charging station in terms of the size and type of EVSEs. These include 10 criteria in Table 1 which are described as either benefit or cost perspectives to allow quantitative evaluations. Using linguistic terms, the degree of importance for each criterion is evaluated individually by a group of experts including a utility manager who supervises a workplace charging station. The Pareto solutions for nine criteria out of ten (except C_9) presented are calculated by the MOO model.

Peak demand, C_1, is one of the key considerations for workplaces [42]. It refers to the contribution of total EV charging loads to peak demand of the facility. It was shown that the charging loads can increase the facility's peak demand significantly [14]. The charging load that causes peak demand to exceed the facility's highest average energy consumption in 15-minute intervals will result in increased monthly demand charges [3], and hence, network losses. The distribution of Pareto optimal solutions of peak demand for a group of 100 EVs with respect to EVSE types considered is shown in Fig. 2.a. As shown, DCFCs achieves lower peak powers while AC EVSE types show relatively higher peak demand behaviors. However, it is also observed

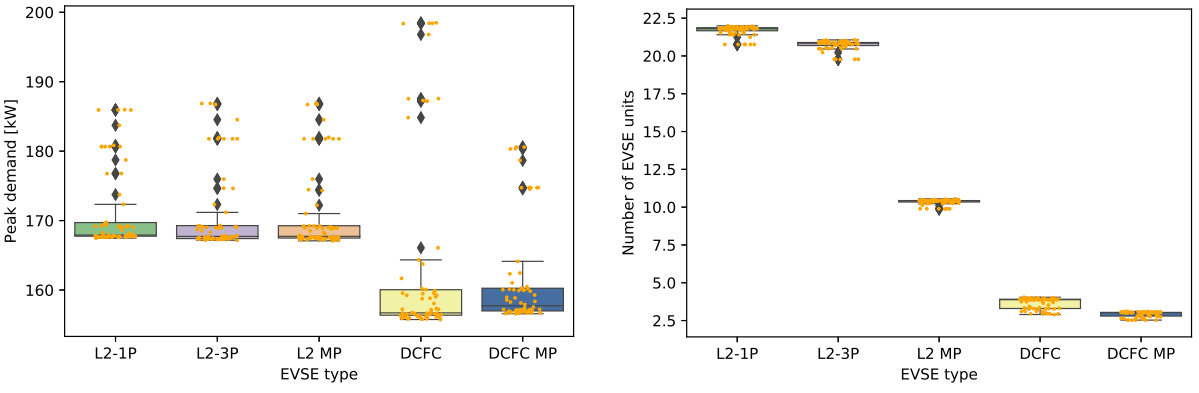

Figure 2: Distribution of Pareto optimal values of the decision-making variables C1 and C2 for 100 EVs with respect to EVSE types, (a) peak demand of aggregated load profiles, (b) EVSE unit numbers (Results are average values over 100 random trials).

that the peak demand can be the highest with DCFCs. Therefore, a suitable MCDM analysis is needed. The number of EVSE units, C_2, refers to the number of charging units to be installed in a workplace EV charging station. It is considered for both cost and benefit perspectives separately. It is practically observed that EVs occupy EVSE more than their required charging time since they need to be plugged off after having been charged due to current EVSE technology. That requires one to monitor charging process and manage the occupancy of EVSEs. In this sense, higher number of EVSE units may be desirable as it increases accessibility for EVs at the same time. However, increasing number of EVSE units depends on site limitations and might require considerable electrical upgrades that will increases EVSE installation costs significantly. As shown in Fig. 2.b, DCFCs require significantly lower number of charging units as compared to AC EVSE types. L2-1P and L2-3P type display close performance in terms of the unit number. Multi-port option reduces the need of charging units significantly for AC EVSE types while it changes slightly for DCFCs.

All cost elements as objectives of the MOO cost model for a given workplace charging environment are considered in the decision-making. Fig. 3 exhibits the distribution of Pareto optimal values of the cost elements considered for a group of 100 EVs. Under the scheduling policy and TOU tariff considered, it is found that DCFC shows better energy charge performance due to better utilization of lower TOU periods with higher charging capacities. AC EVSE types display similar energy charge performances even though they differ from charging powers. This is due to inefficient use of L2-3P capacity (i.e., 22kW) which is much larger than the on-board charger rates of the EVs. Demand charge performances are obtained as similar to that of peak demand as the demand charge is product of demand power and a fixed rate. In terms of EVSE cost, L2-1P shows the best cost performance due to the lowest infrastructure cost even though it requires the highest unit number. L2-3P shows worse performance than that of DCFC types due to higher unit number required.

EVSE occupancy is another key consideration when determining optimal EVSE configuration. It refers to how much time an EV is required to connect to EVSE unit with respect to the required time to complete its charging need. The occupancy is expressed by

$$\mathrm{EVSE}_{\mathrm{occupancy}} = mean\left(\frac{t_{\mathrm{plug-off,i}} - t_{\mathrm{plug-in,i}}}{t_{\mathrm{req,i}}}\right) \qquad i = 1, ..., n, \tag{13}$$

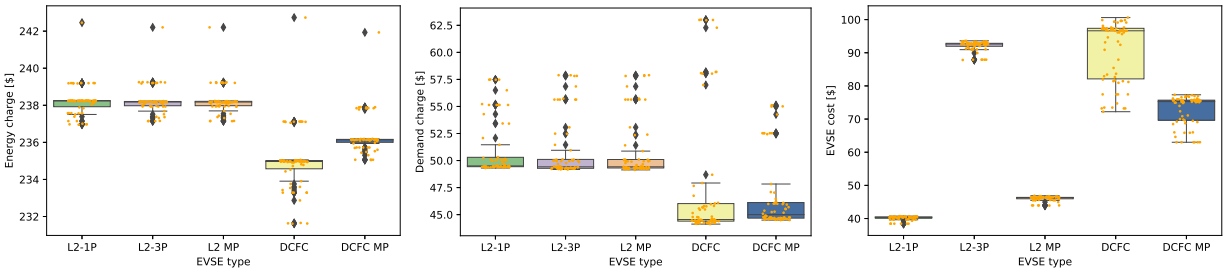

Figure 3: Distribution of Pareto optimal values of the decision-making variables C3, C4, and C5 for 100 EVs with respect to EVSE types, (a) energy charge, (b) demand charge, (c) EVSE cost (Results are average values over 100 random trials).

where, $t_{\text{plug-in,i}}$ and $t_{\text{plug-off,i}}$ are plug-in and plug-off times of i^{th} EV. $t_{\text{req,i}}$ is the required charging time of i^{th} EV that refers to the time needed to achieve desired SOC with the rated charging power. User flexibility is an important consideration for EV users that must be taken into account to guide EVSE selection. It refers to how much time an EV user can leave sooner than the anticipated departure time with the desired SOC.

$$\text{EV}_{\text{flex}} = mean\left(\frac{t_{\text{dept,i}} - t_{\text{plug-off,i}}}{t_{\text{dept,i}} - t_{\text{arr,i}}}\right) \qquad i = 1, ..., n, \tag{14}$$

Among Pareto optimal set, one solution for the three decision variables for 100 EVs is shown in Fig. 4. While % values of the occupancy and user flexibility are used in the calculations, their time values are shown in the figure for convenience. As expected, DCFCs offer the lowest required charging time that increases the user flexibility significantly. AC EVSE types give similar required charging times. The average charging time required for AC EVSE type is increased by approximately 8-fold as compared to DCFC type. Employing an interrupted charging profile requires that EVs are connected to EVSEs more than their required charging times since the algorithm impose charging process at the lower TOU periods and the peak demand. The average occupancy rate for DCFC is found to be approximately 2.8 per vehicle while it ranges 1.6 for AC EVSE types. Since DCFC has more charging flexibility thanks to its higher rated power, the algorithm seeks optimal time slots to minimize both energy and demand charges. This requires EVs to be connected to EVSEs more than their required charging times. However, the user flexibility remains highest with DCFCs. The average flexibility rate per vehicle for DCFC is found to be more than double the rate for AC EVSE types.

Hosting capacity is considered to measure actual EV hosting capacity of an EVSE unit. It is defined as the ratio of the total charging energy provided to total energy capacity of installed EVSE units in the available time horizon by

$$\text{HC} = \frac{\sum_{i}^{n} E_{required}(i)}{S_j(i) \cdot \int_{min(tarr(1:n))}^{max(tdept(1:n))} (P_j^{rated} \cdot \eta_j)\, \mathrm{d}t}. \tag{15}$$

The closer HC is to unity, the better EVSE's capacity use. HC depends on number of EVs. For a group of 100 EVs, distribution of Pareto optimal values of the HC is shown in Fig 5. The multi-port DCFC achieves the highest HC followed by DCFC while L2-3P EVSEs have considerably the lowest HC value. This is due to inefficiency of L2-3P EVSE capacities by the on-board charger specifications of EVs on the market. In

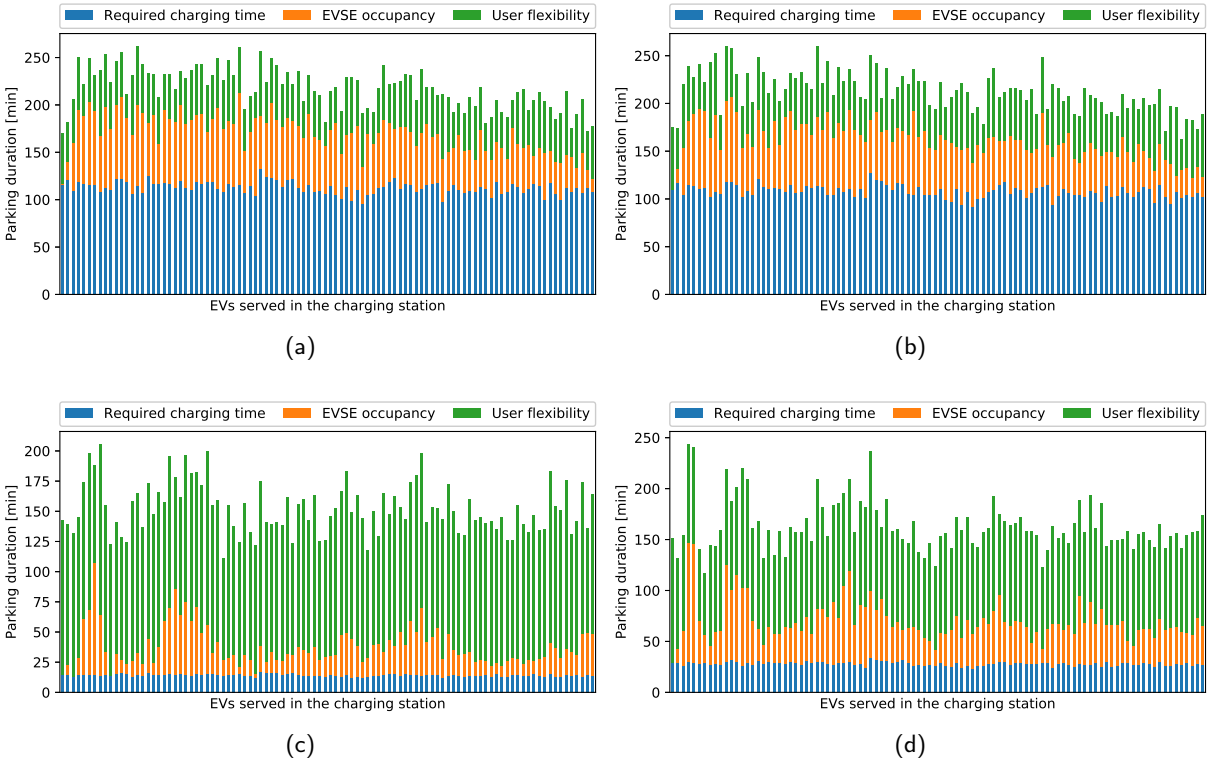

Figure 4: One of the Pareto optimal solutions of the decision-making variables C6, C7, and C10 for 100 EVs with respect to EVSE types, (a) L2-1P, (b) L2-3P, (c) DCFC, (d) Multi-port DCFC (Values are averaged over 100 random trials.).

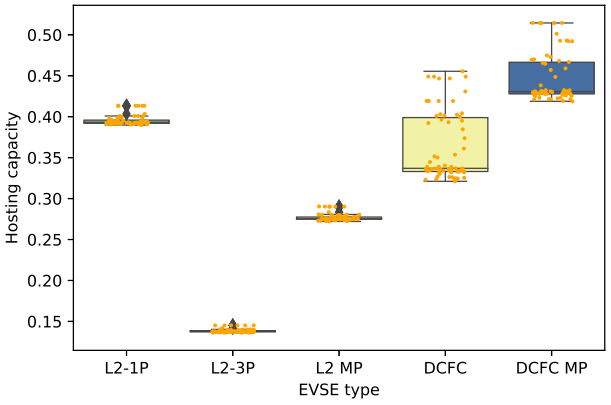

Figure 5: Distribution of Pareto optimal values of hosting capacity (C8) for 100 EVs with respect to EVSE types.

this respect, L2-1P shows closer hosting performance to that of DCFCs. Finally, the lifetime of EVSE unit is considered to help guide EVSE selection. It refers to the operational life cycle of an EVSE unit. A life cycle of 10 is considered for AC EVSE types while the lifetime of DCFC EVSEs are assumed to be 15 years.

4.2. MCDM model development

4.2.1. Dombi operations

Definition 1. *Let ζ_1 and ζ_2 be any two real numbers. Then, the Dombi T-norm and T-conorm between ζ_1 and ζ_2 are defined, respectively as follows [43]:*

$$T_D(\zeta_1,\zeta_2)=\frac{1}{1+\left\{\left(\frac{1-\zeta_1}{\zeta_1}\right)^{\delta}+\left(\frac{1-\zeta_2}{\zeta_2}\right)^{\delta}\right\}^{\frac{1}{\delta}}}, \tag{16}$$

$$T_D^c(\zeta_1,\zeta_2)=1-\frac{1}{1+\left\{\left(\frac{1-\zeta_1}{\zeta_1}\right)^{\delta}+\left(\frac{1-\zeta_2}{\zeta_2}\right)^{\delta}\right\}^{\frac{1}{\delta}}}, \tag{17}$$

where, $\delta>0$ and $\zeta_1,\zeta_2\in[0,1]$.

According to the Dombi T-norm and T-conorm, we define the Dombi operations:

Definition 2. *Suppose ζ_1 and ζ_2 are two real numbers, $\delta,\theta>0$, let it be $f(\zeta_1)=\zeta_1/\sum_{i=1}^{n}\zeta_1$ a real function, then some operational laws of real numbers based on the Dombi T-norm and T-conorm can be defined as follows:*

(1) Addition "+"

$$\zeta_1+\zeta_2=(\zeta_1+\zeta_2)-\frac{\zeta_1+\zeta_2}{1+\left\{\left(\frac{f(\zeta_1)}{1-f(\zeta_1)}\right)^{\delta}+\left(\frac{f(\zeta_2)}{1-f(\zeta_2)}\right)^{\delta}\right\}^{\frac{1}{\delta}}} \tag{18}$$

(2) Multiplication "×"

$$\zeta_1\times\zeta_2=(\zeta_1+\zeta_2)-\frac{\zeta_1+\zeta_2}{1+\left\{\left(\frac{1-f(\zeta_1)}{f(\zeta_1)}\right)^{\delta}+\left(\frac{f(1-\zeta_2)}{f(\zeta_2)}\right)^{\delta}\right\}^{\frac{1}{\delta}}} \tag{19}$$

(3) Scalar multiplication, where $\theta>0$

$$\theta\times\zeta_1=\zeta_1-\frac{\zeta_1}{1+\left\{\theta\left(\frac{f(\zeta_1)}{1-f(\zeta_1)}\right)^{\delta}\right\}^{\frac{1}{\delta}}} \tag{20}$$

(4) Power, where $\theta>0$

$$\zeta_1^{\theta}=\frac{\zeta_1}{1+\left\{\theta\left(\frac{1-f(\zeta_1)}{f(\zeta_1)}\right)^{\delta}\right\}^{\frac{1}{\delta}}} \tag{21}$$

4.2.2. Bonferroni Mean Operators

Definition 3. *[44] Let $(\zeta_1, \zeta_2, \ldots, \zeta_n)$ be a set of non-negative numbers, $\mu_1, \mu_2 \geq 0$, $w_i (i = 1, 2, \ldots, n)$ the relative weight of ζ_i, $w_i \in [0, 1]$ and $\sum_{i=1}^{n} w_i = 1$. If*

$$NWBM^{\mu_1,\mu_2}(\zeta_1, \zeta_2, \ldots, \zeta_n) = \left(\sum_{i,j=1}^{n} \frac{w_i w_j}{1 - w_i} \zeta_i^{\mu_1} \zeta_j^{\mu_2} \right)^{\frac{1}{\mu_1 + \mu_2}}, \tag{22}$$

then, $NWBM^{\mu_1,\mu_2}$ is called to be a normalized weighted Bonferroni mean (NWBM) operator.

Definition 4. *[44] Let $(\zeta_1, \zeta_2, \ldots, \zeta_n)$ be a set of non-negative numbers, $\mu_1, \mu_2 \geq 0$, $w_i (i = 1, 2, \ldots, n)$ the relative weight of ζ_i, $w_i \in [0, 1]$ and $\sum_{i=1}^{n} w_i = 1$. Furthermore, if we write*

$$NWGBM^{\mu_1,\mu_2}(\zeta_1, \zeta_2, \ldots, \zeta_n) = \frac{1}{\mu_1 + \mu_2} \prod_{i,j=1}^{n} \left(\mu_1 \zeta_i + \mu_2 \zeta_j \right)^{\frac{w_i w_j}{1 - w_i}}, \tag{23}$$

then, $NWGBM^{\mu_1,\mu_2}$ is called a normalized weighted geometric Bonferroni mean ($NWGBM$) operator.

4.2.3. Dombi Bonferroni WASPAS Method

Suppose that a MCDM model is defined with m alternatives (A_i) and n criteria (C_j) Then, based on the preliminary settings, we can define the algorithm for the application of the Dombi Bonferroni Weighted Aggregated Sum Product Assessment (WASPAS) methodology, which is presented as follows.

Step 1. Formation of initial decision matrix and normalization of the initial decision matrix. Based on the research problem, the elements of the initial decision matrix $\Phi = \left[\omega_{ij}\right]_{mxn}$ are defined, where the element of the initial matrix ω_{ij} represents the value of the alternative A_i in relation to the criterion C_j. By applying expression (24), the elements of the initial decision matrix are normalized. Thus, we obtain a normalized matrix $\Phi^N = \left[\varpi_{ij}\right]_{mxn}$.

$$\varpi_{ij} = \begin{cases} \varpi_{ij} = \frac{\omega_{ij}}{\varpi_j^+} & \text{if } j \in \text{Benefit} \\ \varpi_{ij} = \frac{\varpi_j^-}{\omega_{ij}} & \text{if } j \in \text{Cost} \end{cases}, \tag{24}$$

where, $\varpi_j^+ = max(\omega_{ij})\ \forall i$ and $\varpi_j^- = min(\omega_{ij})\ \forall i$.

Step 2. Determination of weight coefficients of criteria. The weighting coefficients of the criteria are defined by applying a logarithmic additive evaluation of expert estimates. Experts $(\Omega_1, \Omega_2, \ldots, \Omega_b)$ evaluate the criteria to define the priority vector $\Theta^t = \left(\gamma_{C1}^t, \gamma_{C2}^t, \ldots, \gamma_{Cn}^t\right)$, $1 \leq t \leq b$.

Step 2.1. To define the relation vector, Ψ^t, applying the condition $\tau_{AIP} < min\left(\gamma_{C1}^t, \gamma_{C2}^t, \ldots, \gamma_{Cn}^t\right)$ defines the absolute anti-ideal point (τ_{AIP}). Using expression (25), the relationship between the elements of the priority vector and the absolute anti-ideal point is determined.

$$\rho_{Cn}^t = \frac{\gamma_{Cn}^t}{\tau_{AIP}}, \tag{25}$$

where, ρ_{Cn}^t represents the element of the relation vector $\Psi^t = \left(\rho_{C1}^t, \rho_{C2}^t, \ldots, \rho_{Cn}^t\right)$, $1 \leq t \leq b$.

Step 2.2. Determination of the final vector of the weight coefficients $w_j = \left(w_1, w_2, \ldots, w_n\right)^T$. By applying expression (26), we obtain the values of the weighting coefficients of the criteria for the expert, t, $(1 \leq t \leq b)$.

$$w_j^t = \frac{ln\left(\rho_{Cn}^t\right)}{ln\left(v^t\right)}, \tag{26}$$

where, ρ_{Cn}^{t} represents the elements of the relation vector $\Psi^{t} = \left(\rho_{C1}^{t}, \rho_{C2}^{t}, \ldots, \rho_{Cn}^{t}\right)$, while $v^{t} = \prod_{j=1}^{n} \rho_{Cn}^{t}$.

Using the Dombi weighted operator in (27), we obtain an aggregate vector of the weight coefficients.

$$w_j = \frac{\sum_{j=1}^{b} w_j}{1 + \left\{ \sum_{j=1}^{b} \frac{1}{b} \left(\frac{1 - f(w_j)}{f(w_j)} \right)^{\delta} \right\}^{1/\delta}}, \tag{27}$$

where, $f\left(w_j\right) = w_j / \sum_{j=1}^{b} w_j$ represents a function of the weighting factor, while b represents the total number of experts.

Step 3. Calculation of weight sum and product for alternatives. Using the Dombi T-norm and T-conorm and the Bonferroni operators in (22) and (23), weighted sequences of alternatives are specified. Based on *Definitions 1, 2, 3,* and *4*, we can define Dombi Bonferroni weighted averaging function (DBW_i) and Dombi Bonferroni weighted geometric function (DBG_i) as follow.

Theorem 1. Let $\varpi_{ij} (j = 1, 2, \ldots, n)$ be a set of matrix elements $\Phi^{N} = \left[\varpi_{ij}\right]_{mxn}$ and let $\mu_1, \mu_2, \delta \geq 0$. If we denote $w_j = \left(w_1, w_2, \ldots, w_n\right)^{T}$ the vector of the weight coefficients of the criteria, then we can represent the DBW_i function as follow:

$$DBW_i^{\mu_1,\mu_2,\delta} = \left(\frac{w_i w_j}{1 - w_i} \sum_{i,j=1(i \neq j)}^{n} \varpi_i^{\mu_1} \varpi_j^{\mu_2} \right)^{\frac{1}{\mu_1 + \mu_2}} = \frac{\sum_{j=1}^{n} \varpi_j}{1 + \left\{ \frac{1}{w_i w_j (\mu_1 + \mu_2)} \frac{1 - w_i}{\sum_{i,j=1(i \neq j)}^{n} \frac{1}{\mu_1 \left(\frac{1 - f(\varpi_i)}{f(\varpi_i)} \right)^{\delta} + \mu_2 \left(\frac{1 - f(\varpi_j)}{f(\varpi_j)} \right)^{\delta}}} \right\}^{1/\delta}}, \tag{28}$$

where, $w_j = \left(w_1, w_2, \ldots, w_n\right)^{T}$ is the vector of the weight coefficients of the criteria, while $f\left(\varpi_i\right) = \varpi_j / \sum_{j=1}^{n} \varpi_j$. The proof of *Theorem 1* is given in *Appendix* A.

Theorem 2. Let $\varpi_{ij} (j = 1, 2, \ldots, n)$ be a set of matrix elements $\Phi^{N} = \left[\varpi_{ij}\right]_{mxn}$ and let $\mu_1, \mu_2, \delta \geq 0$. If we denote $w_j = \left(w_1, w_2, \ldots, w_n\right)^{T}$ the vector of weight coefficients of the criteria, then we can represent the DBG_i function as follow:

$$DBG_i = \left(\frac{1}{\mu_1 + \mu_2} \prod_{i,j=1}^{n} \mu_1 \varpi_i + \mu_2 \varpi_j \right)^{\frac{w_i w_j}{1 - w_i}} = \sum_{j=1}^{n} \varpi_j - \frac{\sum_{j=1}^{n} \varpi_j}{1 + \left\{ \frac{1}{w_i w_j (\mu_1 + \mu_2)} \frac{1 - w_i}{\sum_{i,j=1(i \neq j)}^{n} \frac{1}{\mu_1 \left(\frac{1 - f(\varpi_i)}{f(\varpi_i)} \right)^{\delta} + \mu_2 \left(\frac{1 - f(\varpi_j)}{f(\varpi_j)} \right)^{\delta}}} \right\}^{1/\delta}}, \tag{29}$$

where, $w_j = \left(w_1, w_2, \ldots, w_n\right)^{T}$ is the vector of the weight coefficients of the criteria, while $f\left(\varpi_i\right) = \varpi_j / \sum_{j=1}^{n} \varpi_j$. The proof of *Theorem 2* is provided in *Appendix* B.

Step 4. Calculation of the integrated value of the Dombi Bonferroni functions, (χ_i) can be expressed by

$$\chi_i = \frac{\zeta \cdot DBW_i + (1 - \zeta) DBG_i}{\sum_{i=1}^{n} \left(\zeta \cdot DBW_i + (1 - \zeta) DBG_i \right)}, \zeta \in \left[0, 1\right]. \tag{30}$$

The coefficient ζ defines the intensity of the influence of DBW_i and DBG_i functions on the final decision. When defining the initial solution, the value of 0.5 is more often adopted. This ensures equal intensity of influence of both Dombi Bonferroni functions.

Step 5. Alternatives are ranked based on their integrated values of the Dombi Bonferroni functions. The closer χ_i is to unity, the better alternative's performance.

Table 2
Best performing Pareto optimal indices for the EVSEs considered.

	L2-1P	L2-3P	L2 MP	DCFC	DCFC MP
Pareto index	66	66	66	45	51

Table 3
Initial decision matrix for the EVSEs considered.

Criteria	L2-1P	L2-3P	L2MP	L3	L3MP
C1	183.723	184.528	184.528	184.828	174.746
C2	21.240	20.230	10.115	2.900	2.530
C3	242.459	242.203	242.203	232.869	235.721
C4	56.496	56.852	56.852	56.985	52.525
C5	39.335	89.915	44.957	72.221	63.007
C6	1.622	1.633	1.633	2.781	2.632
C7	112.884	108.116	108.116	14.307	28.128
C8	0.403	0.142	0.283	0.455	0.514
C9	10	10	10	15	15
C10	11.836	12.697	12.697	26.119	21.394

5. Experimental results

5.1. Results for alternatives

The application of the Dombi Bonferroni WASPAS method for determining the optimal EVSE configuration has been performed in the two phases. First, the Dombi Bonferroni WASPAS method has been applied to find the best performing Pareto solution among 66 optimal solutions for each EVSE type considered. Table 2 reports the Pareto indices identified.

In the second phase, the Dombi Bonferroni WASPAS method has been applied to rank the best performing solutions of the alternatives as follow:

Step 1: The initial decision matrix $\Phi = \left[\omega_{ij}\right]_{5x10}$ was formed and its elements were normalized using expression (24) that is presented in Table 3.

Then, using (24) the elements of the matrix Φ, ω_{ij}were transformed into standardized values ($\varpi_{ij}$from the interval $\varpi_{ij} \in \left[0,1\right]$. Thus, the elements of the normalized matrix $\Phi^N = \left[\varpi_{ij}\right]_{5x10}$ were obtained as shown in Table 4.

Step 2: Weighting coefficients of the criteria were defined by applying logarithmic additive evaluation of expert assessments. Four experts $\Omega = \left\{\Omega_1, \Omega_2, \Omega_3, \Omega_4\right\}$ participated in the study and evaluated the criteria based on the seven-point scheme: Very low (VL) - 1, Low (L) - 2, Medium-low (ML) - 3, Medium (M) - 4, Medium-high MH) - 5, High (H) - 6, Very high (VH) - 7. Based on expert assessments, priority vectors for each expert were defined individually that is reported in Table 5.

Step 2.1: Based on the condition that $\tau_{AIP} < min\left(\gamma_{C1}^t, \gamma_{C2}^t, \ldots, \gamma_{Cn}^t\right)$, the absolute anti-ideal point $\tau_{AIP} = 0.5$ was defined. Using the expression (25), the relations between the elements of the priority vector in Table 5, and the absolute anti-ideal point (τ_{AIP}) were defined as in Table 6.

Step 2.2: Using the expression (26), the weighting coefficients of the criteria for each expert were obtained as reported in Table 7. Using the Dombi weighted function, (27), a fusion of the weighting coefficients obtained for the experts was performed. When applying the Dombi weighted function, the value of the parameter $\delta = 1$ was adopted. As an example, the fusion of the value for the weight coefficient w_1 in Table 7 was performed as follows:

Table 4
Normalized matrix of the EVSEs considered.

Criteria	L2-1P	L2 MP	L2-3P	DCFC	DCFC MP
C1	0.951	0.947	0.947	0.945	1.000
C2	0.119	0.250	0.125	0.872	1.000
C3	0.960	0.961	0.961	1.000	0.988
C4	0.930	0.924	0.924	0.922	1.000
C5	1.000	0.875	0.437	0.545	0.624
C6	1.000	0.993	0.993	0.583	0.616
C7	0.127	0.132	0.132	1.000	0.509
C8	0.784	0.551	0.275	0.885	1.000
C9	0.667	0.667	0.667	1.000	1.000
C10	0.453	0.486	0.486	1.000	0.819

Table 5
Criteria priority vectors of the experts.

Criteria	Expert-1	Expert-2	Expert-3	Expert-4
C1	M	MH	H	VH
C2	H	MH	H	MH
C3	M	L	M	MH
C4	M	MH	MH	VH
C5	ML	M	ML	M
C6	H	M	MH	MH
C7	H	M	H	H
C8	H	M	MH	H
C9	H	L	M	M
C10	M	MH	M	M

Table 6
Relationship vectors between the elements of the priority vector and the absolute anti-ideal point.

Criteria	Expert-1	Expert-2	Expert-3	Expert-4
C1	8	10	12	14
C2	12	10	12	10
C3	8	4	8	10
C4	8	10	10	14
C5	6	8	6	8
C6	12	8	10	10
C7	12	8	12	12
C8	12	8	10	12
C9	12	4	8	8
C10	8	10	8	8

$$w_1 = \frac{0.2149+0.2641+0.2584+0.2627}{1+\left\{\frac{1}{4}\left(\frac{1-0.0923}{0.0923}\right)+\left(\frac{1-0.1134}{0.1134}\right)+\left(\frac{1-0.111}{0.111}\right)+\left(\frac{1-0.1128}{0.1128}\right)\right\}^{1/1}} = 0.1066$$

Fusion of the values for the remaining weighting coefficients performed in a similar manner.

Table 7
Criteria weight vectors of the experts

Criteria	Expert-1	Expert-2	Expert-3	Expert-4	Final wj
C1	0.092	0.113	0.111	0.113	0.107
C2	0.110	0.113	0.111	0.098	0.108
C3	0.092	0.068	0.093	0.098	0.086
C4	0.092	0.113	0.103	0.113	0.105
C5	0.080	0.102	0.080	0.089	0.087
C6	0.110	0.102	0.103	0.098	0.103
C7	0.110	0.102	0.111	0.106	0.107
C8	0.110	0.102	0.103	0.106	0.105
C9	0.110	0.068	0.093	0.089	0.087
C10	0.092	0.113	0.093	0.089	0.096

Table 8
Calculated integrated values (χ_i) of the Dombi Bonferroni functions for the optimal EVSE configurations.

	L2-1P	L2-3P	L2 MP	DCFC	DCFC MP
χ_i if C_2 is cost attribute type	0.584	0.482	0.593	0.862	0.835
χ_i if C_2 is benefit attribute type	0.725	0.599	0.635	0.740	0.699

Step 3: The calculations of the weighted sum and the weight product of the alternatives were performed using the funtions DBW_i and DBG_i in (28) and (29), respectively. The values of the parameters $\mu_1 = \mu_2 = \delta = 1$ were adopted in the calculations. The DBW_i and DBG_i functions for the alternatives have been obtained as:

$$DBW_i^{\mu_1=\mu_2=\delta=1} = \begin{bmatrix} 0.580 \\ 0.477 \\ 0.847 \\ 0.819 \\ 0.577 \end{bmatrix}; DBG_i^{\mu_1=\mu_2=\delta=1} = \begin{bmatrix} 0.607 \\ 0.488 \\ 0.878 \\ 0.851 \\ 0.590 \end{bmatrix}$$

Step 4: When calculating the integrated values of the functions in (30), the coefficient ζ of 0.5 was adopted. Hence, the same intensity influence for both Dombi Bonferroni functions in the integrated alternative value was achieved. Finally, the integrated values of the Dombi Bonferroni function for each EVSE type have been obtained as given in Table 8. As discussed in Section 4.1, C2 has two evaluation perspectives, the ranking was done for both perspectives.

The alternatives were ranked with respect to their integrated values of the Dombi Bonferroni functions. The final ranking has been found to be DCFC > DCFC MP > L2 MP > L2-1P > L2-3P. Regarding the expert ranking of criteria, the results in Table 7 reveal that the number of charging units is found to have the highest importance degree followed by required charging time and peak power while energy charge, EVSE cost and its lifetime have the lowest importance degrees. Demand charge, hosting capacity, and EVSE occupancy are other main factors affecting the ranking. The primary reason for DCFC being the best alternative is that it has significantly the lowest required charging time and energy charge while providing the highest user flexibility owing to its relatively higher charging rates. In terms of the number of charging units and hosting capacity, DCFC displays also similar performance to those of multi-port DCFC which has the best values. One of the highest importance factor, C_7 brings down the score of DCFC MP below that of DCFC, even though it shows

better performance in terms of peak power, the number of EVSE unit, and demand charge. In this respect, it is shown that the cost and lifetime of EVSE units has minor impact on the ranking. While AC EVSE types show similar performances, the difference in the number of EVSE units make L2 MP superior as compared to L2-1P and L2-3P. The major reason for L2-3P being the worst alternative is that it has significantly the lowest hosting capacity due to inefficient use of charging capacity.

When C_2 is evaluated from benefit perspective, the ranking is found to be DCFC >L2-1P>DCFC MP>L2 MP >L2-3P. DCFC is still the best alternative even though it requires the lowest number of EVSE units. While C2 has the most importance degree, DCFC has the lowest charging time which make it superior alternative. In this case, L2-1P outperforms DCFC MP since it provides significantly higher EVSE accessibility owing to having higher unit number. L2 is still found to be the worst alternative due to the lowest hosting capacity and providing less user flexibility.

5.2. Sensitivity analysis

In this section, the robustness of the ranking results obtained is tested to find the most optimum EVSE type from the charging station owner perspective. To date, the literature has not adopted a single methodology for checking the robustness of results in MCDM problems. One reason is due to the specifics of the MCDM method used and the nature of the problem to be solved. Several authors [45, 46] claim that it is necessary to analyze the influence of subjectively defined input parameters of model on decision-making. In the proposed Dombi Bonferroni WASPAS model, there are four parameters (ζ, μ_1, μ_2, and δ) that are defined based on the subjective preferences of decision makers. Therefore, the robustness of the solution is analyzed for a set of varying values of the parameters ζ, μ_1, μ_2, and δ.

5.2.1. Impact of coefficient ζ on the ranking

Based on the value of the coefficient ζ, the degree of influence of the Dombi Bonferroni function on the final decision is firstly defined. In the presented results, a value of $\zeta = 0.5$ for the coefficient was already used, which achieved equal influence of both Dombi Bonferroni functions. To consider the influence of the coefficient ζ on the final decision, 11 different scenarios were formed for which the change of the coefficient ζ in the interval [0, 1] was simulated. In the initial scenario, the value $\zeta = 0.0$ was adopted, giving preference to the DBG_i function (30), while in each subsequent scenario, an increment of 0.1 was adopted. As such, by increasing the coefficient ζ by 0.1, the intensity of the influence of the DBW_i function was increased by 10%. At the same time, the intensity of the impact of the DBG_i function was reduced by 10%. This has resulted in a reduction in the integrated functions of alternatives. The dependence of the integrated alternative functions on varying values of the coefficient ζ is shown in Fig. 6. As shown, an increase in the value of the coefficient $0 \leq \zeta \leq 1$ affects the decrease in the Dombi Bonferroni function. The values of the DBW_i function have smaller values compared to those of the DBG_i function. It is also observed that the intensity of decreasing of the integrated alternative functions is gradual and there are no drastic changes that can lead to a change in the ranking of the alternatives. These results confirm that DCFC EVSE is the best performing solution as it has a distinct dominance over other EVSE types in the set of alternatives.

5.2.2. Impact of coefficients μ_1, μ_2, and δ on the ranking

As the parameters μ_1, μ_2 and δ affect directly the values of the Dombi Bonferroni function, it is necessary to examine whether or not the changes in the Dombi Bonferroni function for all alternatives are proportional, i.e., uniform. If the Dombi Bonferroni functions of alternatives increase faster or slower due to a change in the parameters, there may be a change in the ranking. To explore this, two experiments have been performed in which the change of parameters μ_1, μ_2 and δ in the interval $1 \leq \mu_1, \mu_2, \delta \leq 100$ was simulated. In the first experiment, keeping $\mu_1 = \mu_2 = 1$, the change of parameter $1 \leq \delta \leq 100$ was simulated, while the second includes the simulation runs for change of both parameters $1 \leq \mu_1, \mu_2 \leq 100$ by keeping $\delta = 1$. Thus,

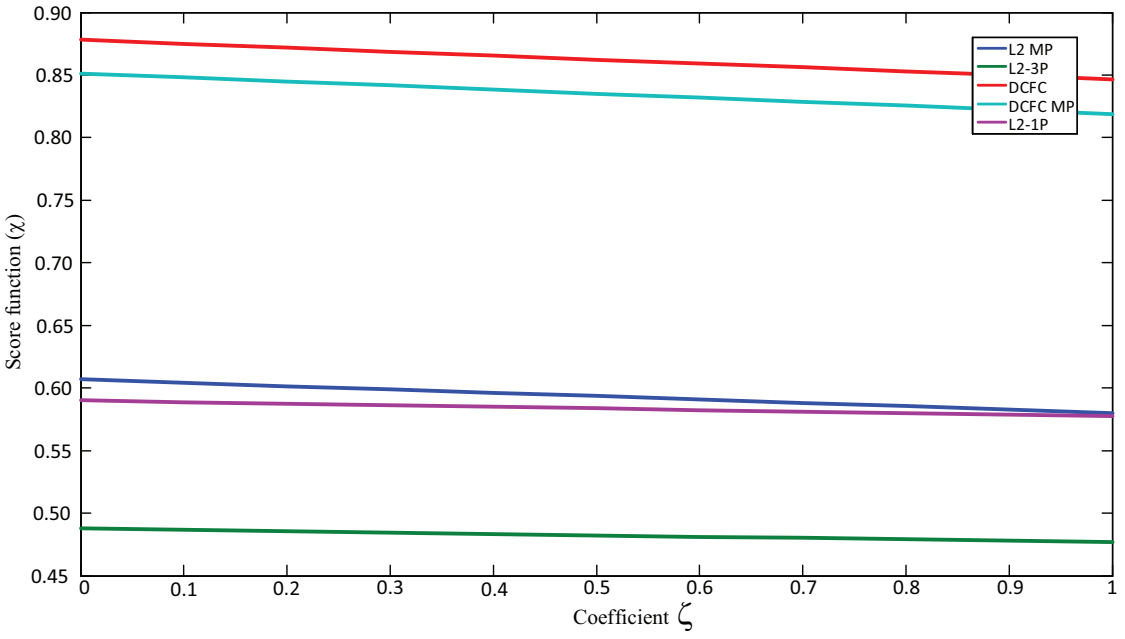

Figure 6: Behavior of the integrated value of Dombi Bonferroni functions for varying values of $\zeta \in [0, 1]$ for the optimal EVSE configurations.

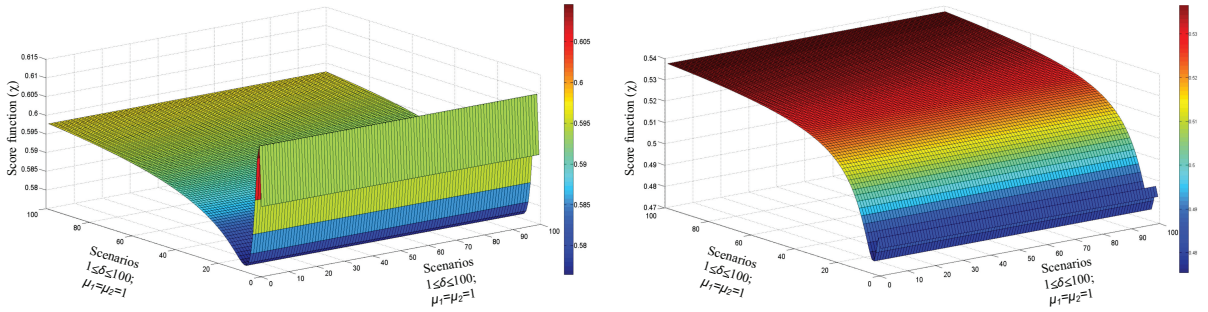

(a) (b)

Figure 7: Behavior of the integrated value of Dombi Bonferroni functions for varying values of $\delta \in [1, 100]$, (a) L2 MP and (b) L2-3P EVSE types.

100 scenarios were considered in each experiment, during which the dependence of integrated alternative functions on the change of the parameters was examined.

As an example, Fig. 7 shows the first experiment results for L2-3P and L2 MP EVSE types. Similar changes have been obtained for other alternatives. The behaviors of the Dombi Bonferroni funtion integrated values for all EVSE types is shown in Fig. 8. It is clearly seen that the change of the parameters $1 \leq \delta \leq 100$ significantly affects the change of the integrated values of the Dombi Bonferroni function. However, it is observed that there is no drastic changes in the integrated values that can lead to any change in the ranking of the alternatives. This experiment confirms the initial ranking result that is DCFC> DCFC MP> L2 MP> L2-1P> L2-3P while DCFC is the best solution.

In the second experiment, the change of the parameters $1 \leq \mu_1, \mu_2 \leq 100$ has been simulated. In each scenario, the parameters μ_1 and μ_2 were assigned to the same values. As such, in the first scenario, the

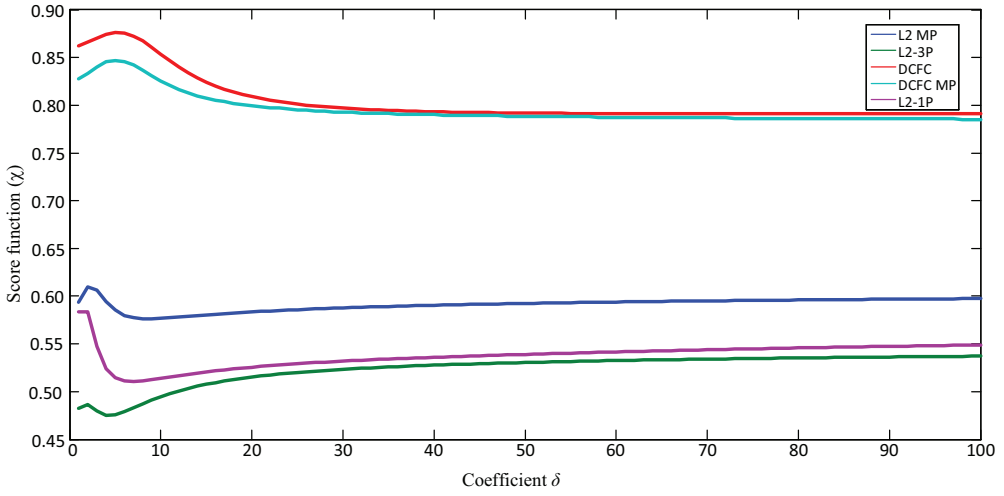

Figure 8: Behavior of the integrated value of Dombi Bonferroni functions for varying δ values [1 100] for the optimal EVSE considerations.

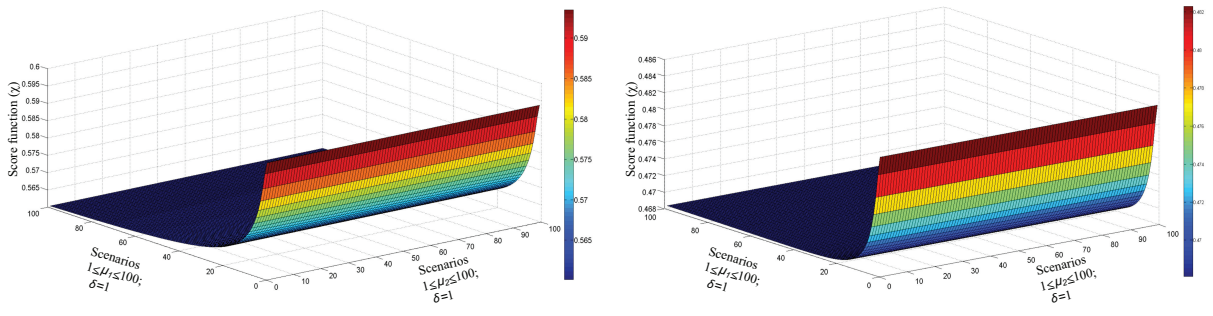

(a) (b)

Figure 9: Behavior of the integrated value of Dombi Bonferroni functions for varying values of $\mu_1, \mu_2 \in [1, 100]$, (a) L2 MP and (b) L2-3P EVSE types.

parameter value $\mu_1 = \mu_2 = 1$ is adopted. Then, the value of the parameters was increased by one in each subsequent scenario. As an example, Fig. 9 shows the dependence of the integrated values of the Dombi Bonferroni functions for L2-3P and L2 MP EVSEs. Similar changes occur in the behaviors of other EVSE types. Fig. 10 displays a comparative overview of the change in the integrated values for each EVSE types considered. As shown, it is confirmed that the change of the parameters μ_1, μ_2 affects significantly the change of the integrated values of the Dombi Bonferroni functions. However, the changes happen proportionally for each alternative across the scenarios that do not change the ranking of the alternatives. It can be concluded that the valid ranking is to be DCFC> DCFC MP> L2 MP> L2-1P> L2-3P.

5.3. Comparative analysis

To validate the ranking result from the proposed method, it has been compared with other MCDM models, including traditional WASPAS [47], MABAC [48], MAIRCA [49], and CoCoSo [50] methods. These methods were implemented since they differ in the way of normalizing the data, which can significantly

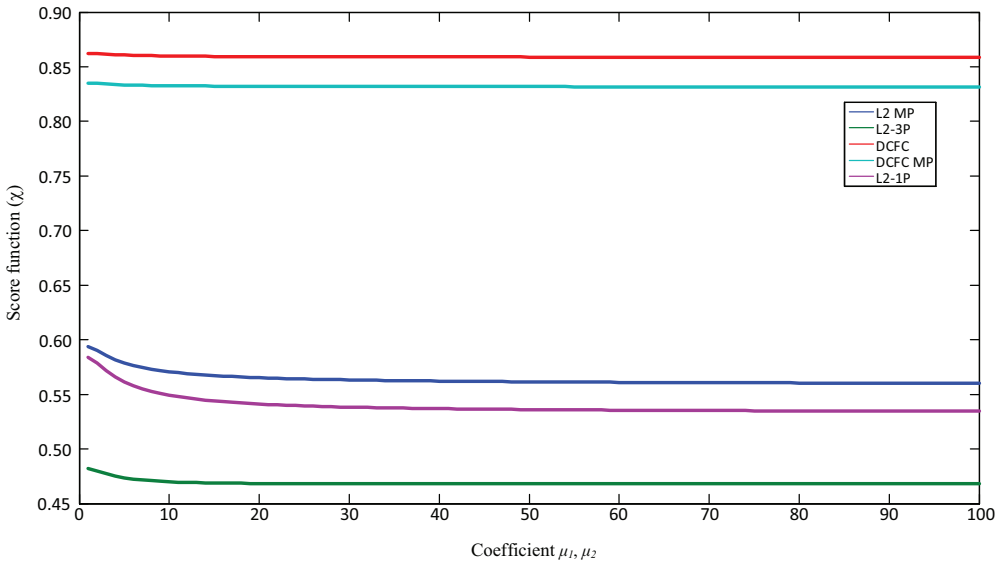

Figure 10: Behavior of the integrated value of Dombi Bonferroni functions for varying μ_1 and μ_2 values [1 100] for the optimal EVSE considerations.

Table 9
Comparison of the rankings with various MCDM methods.

	L2-1P	L2-3P	L2 MP	DCFC	DCFC MP
Proposed method	4	5	3	1	2
WASPAS	4	5	3	1	2
MABAC	3	5	4	1	2
MAIRCA	3	5	4	1	2
CoCoSo	4	5	3	1	2

affect the ranking of alternatives [51, 52]. After implementing each model individually, the ranking results are obtained as summarized in Table 9.

It has been observed that the MCDM models implemented yielded very similar ranking results for each alternative. DCFC is the best performing optimal configuration followed by DCFC MP while L2-3P is the least feasible EVSE option for all approaches. The only difference found between the methodologies was how the MABAC and MAIRCA methods ranked L2-1P and L2 MP EVSEs. However, based on the experts' experience with EVSEs, L2 MP should in fact be a better alternative relative to L2-1P thanks to its relatively less number of charging units and required charging time while both EVSE types displays very similar performance for all aspects considered. Therefore, consistency with the majority of the MCDM models and this additional expert validation serves to verify the reliability of the proposed model.

As compared to the MCDM methods considered, the main features of the proposed model that make it outperformed can be summarized as follow. The Dombi Bonferroni based WASPAS model allows the input parameters support each other. Furthermore, it can be applied to decision makers with different risk attitudes based on flexible parameters. It can also eliminate the influence of extreme values from the decision matrix. the Dombi Bonferroni WASPAS method differs from its counterparts for defining the relationships among the decision variables thanks to the application of the logarithmic additive function and Dombi norms. That is why it is a fully defined multi-criteria framework that enables the definition of criterion weights and the

evaluation of alternatives. It can therefore be concluded that the Dombi Bonferroni WASPAS method is more suitable for solving realistic decision-making problems.

6. Conclusion

This study has presented an integrated multi-objective optimization and multi-criteria decision-making model to find the optimal EVSE configuration at workplaces. In the proposed approach, a multi-objective optimization model for a given workplace charging station is first presented that yields the Pareto solutions. To select the best performing solution, the Pareto frontier is then evaluated by a proposed multi-criteria decision-making model in which charging station operator's perspectives are included in weighting the decision-making variables. The proposed multi-criteria decision-making model is an improved version of conventional WASPAS method in which the Dombi Bonferroni fuctions are introduced for determining the weight coefficients of the decision-making variables. Once the best performing Pareto points are identified for all possible EVSE configurations, in the last step, the selected EVSE configurations are ranked by implementing the proposed multi-criteria decision-making model. The ranking results have been validated by comparing with those of other four state-of-the-art methods. Finally, a sensitivity analysis has been performed to test the robustness of the ranking results.

Based on the workplace mobility pattern considered, the proposed integrated model chose DCFC as the best EVSE option while L2-3P EVSE was found to be the least attractive option. The ranking order for the other alternatives was found to be DCFC MP>L2 MP>L2-1P. The results demonstrate that the inclusion of the multi-objective optimization model outputs into the decision-making process can reveal distinguishing features in EVSE types. As a result, the proposed approach has identified a different ranking order than the traditional EVSE selection practices at workplaces in which L2 MP types are typically installed. Moreover, the comparison analysis revealed a consistency among the results of the implemented multi-criteria decision-making models. However, the proposed model is superior in terms of flexibility enabling the definition of weights for decision-making variables and thus the evaluation of alternatives. The sensitivity analysis also revealed that the ranking remains the same in response to changes of weightings of the model coefficients.

Appendix A

The proof of *Theorem 1*:

The expression (22) can be decomposed into segments in order to gradually derive expression (28). From Expression (22), we get that:

$$\varpi_i^{\mu_1} = \frac{\varpi_i}{1+\left\{\mu_1\left(\frac{1-f(\varpi_i)}{f(\varpi_i)}\right)^{\delta}\right\}^{1/\delta}} \; ; \; \varpi_j^{\mu_2} = \frac{\varpi_j}{1+\left\{\mu_2\left(\frac{1-f(\varpi_j)}{f(\varpi_j)}\right)^{\delta}\right\}^{1/\delta}}.$$

Next, we get that

$$\varpi_i^{\mu_1}\varpi_j^{\mu_2} = \frac{\varpi_i^{\mu_1}+\varpi_j^{\mu_2}}{1+\left\{\mu_1\left(\frac{1-f(\varpi_i)}{f(\varpi_i)}\right)^{\delta}+\mu_2\left(\frac{1-f(\varpi_j)}{f(\varpi_j)}\right)^{\delta}\right\}^{1/\delta}},$$

followed by

$$\sum_{i,j=1(i\neq j)}^{n}\varpi_i^{\mu_1}\varpi_j^{\mu_2} = \sum_{j=1}^{n}\varpi_j - \frac{\sum_{j=1}^{n}\varpi_j}{1+\left\{\sum_{i,j=1(i\neq j)}^{n}\frac{1}{\mu_1\left(\frac{1-f(\varpi_i)}{f(\varpi_i)}\right)^{\delta}+\mu_2\left(\frac{1-f(\varpi_j)}{f(\varpi_j)}\right)^{\delta}}\right\}^{1/\delta}},$$

and

$$\frac{w_i w_j}{1-w_i}\sum_{i,j=1(i\neq j)}^{n}\varpi_i^{\mu_1}\varpi_j^{\mu_2}=\sum_{j=1}^{n}\varpi_j-\frac{\sum_{j=1}^{n}\varpi_j}{1+\left\{\frac{w_i w_j}{1-w_i}\sum_{i,j=1(i\neq j)}^{n}\frac{1}{\mu_1\left(\frac{1-f(\varpi_i)}{f(\varpi_i)}\right)^{\delta}+\mu_2\left(\frac{1-f(\varpi_j)}{f(\varpi_j)}\right)^{\delta}}\right\}^{1/\delta}},$$

Finally, the DBW_i function is obtained as follow:

$$DBW_i^{\mu_1,\mu_2,\delta}=\left(\frac{w_i w_j}{1-w_i}\sum_{i,j=1(i\neq j)}^{n}\varpi_i^{\mu_1}\varpi_j^{\mu_2}\right)^{\frac{1}{\mu_1+\mu_2}}=\frac{\sum_{j=1}^{n}\varpi_j}{1+\left\{\frac{1}{w_i w_j(\mu_1+\mu_2)}\frac{1-w_i}{\sum_{i,j=1(i\neq j)}^{n}\frac{1}{\mu_1\left(\frac{1-f(\varpi_i)}{f(\varpi_i)}\right)^{\delta}+\mu_2\left(\frac{1-f(\varpi_j)}{f(\varpi_j)}\right)^{\delta}}}\right\}^{1/\delta}}.$$

Appendix B

The proof of *Theorem 2*:

The expression (23) can be decomposed into segments in order to gradually derive the expression (29). From Expression (23) we get that:

$$\mu_1\varpi_i=\frac{\varpi_i}{1+\left\{\mu_1\left(\frac{1-f(\varpi_i)}{f(\varpi_i)}\right)^{\delta}\right\}^{1/\delta}};\ \mu_2\varpi_j=\frac{\varpi_j}{1+\left\{\mu_2\left(\frac{1-f(\varpi_j)}{f(\varpi_j)}\right)^{\delta}\right\}^{1/\delta}}.$$

The summation is

$$\mu_1\varpi_i+\mu_2\varpi_j=\varpi_i+\varpi_j-\frac{\varpi_i+\varpi_j}{1+\left\{\mu_1\left(\frac{1-f(\varpi_i)}{f(\varpi_i)}\right)^{\delta}+\mu_2\left(\frac{1-f(\varpi_j)}{f(\varpi_j)}\right)^{\delta}\right\}^{1/\delta}},$$

followed by

$$\left(\mu_1\varpi_i+\mu_2\varpi_j\right)^{\frac{w_i w_j}{1-w_i}}=\frac{\varpi_i+\varpi_j}{1+\left\{\frac{1}{1-w_i}\frac{w_i w_j}{\mu_1\left(\frac{1-f(\varpi_i)}{f(\varpi_i)}\right)^{\delta}+\mu_2\left(\frac{1-f(\varpi_j)}{f(\varpi_j)}\right)^{\delta}}\right\}^{1/\delta}},$$

and

$$\prod_{i,j=1(i\neq j)}^{n}\left(\mu_1\varpi_i+\mu_2\varpi_j\right)^{\frac{w_i w_j}{1-w_i}}=\frac{\sum_{j=1}^{n}\varpi_j}{1+\left\{\frac{w_i w_j}{1-w_i}\sum_{i,j=1(i\neq j)}^{n}\frac{1}{\mu_1\left(\frac{1-f(\varpi_i)}{f(\varpi_i)}\right)^{\delta}+\mu_2\left(\frac{1-f(\varpi_j)}{f(\varpi_j)}\right)^{\delta}}\right\}^{1/\delta}}.$$

Finally, the DBG_i function is obtained as follow:

$$DBG_i=\frac{1}{\mu_1+\mu_2}\prod_{i,j=1}^{n}\left(\mu_1\varpi_i+\mu_2\varpi_j\right)^{\frac{w_i w_j}{1-w_i}}=\sum_{j=1}^{n}\varpi_j-\frac{\sum_{j=1}^{n}\varpi_j}{1+\left\{\frac{1}{w_i w_j(\mu_1+\mu_2)}\frac{1-w_i}{\sum_{i,j=1(i\neq j)}^{n}\frac{1}{\mu_1\left(\frac{1-f(\varpi_i)}{f(\varpi_i)}\right)^{\delta}+\mu_2\left(\frac{1-f(\varpi_j)}{f(\varpi_j)}\right)^{\delta}}}\right\}^{1/\delta}}.$$

References

[1] Global EV outlook: Entering the decade of electric drive?, https://www.iea.org/reports/global-ev-outlook-2020, 2021. [Online; accessed 01-June-2021].

[2] Y. Huang, Y. Zhou, An optimization framework for workplace charging strategies, Transportation Research Part C: Emerging Technologies 52 (2015) 144–155.

[3] S. Kucuksari, N. Erdogan, "EV specific time-of-use rates analysis for workplace charging", in: 2021 IEEE Transportation Electrification Conference & Expo (ITEC), IEEE, 2021, pp. 783–788.

[4] E. R. Munoz, F. Jabbari, A decentralized, non-iterative smart protocol for workplace charging of battery electric vehicles, Applied Energy 272 (2020) 115187.

[5] J. Zhao, S. Kucuksari, E. Mazhari, Y.-J. Son, Integrated analysis of high-penetration PV and PHEV with energy storage and demand response, Applied Energy 112 (2013) 35–51.

[6] P. Sadeghi-Barzani, A. Rajabi-Ghahnavieh, H. Kazemi-Karegar, Optimal fast charging station placing and sizing, Applied Energy 125 (2014) 289–299.
[7] M. C. Kisacikoglu, F. Erden, N. Erdogan, Distributed control of PEV charging based on energy demand forecast, IEEE Transactions on Industrial Informatics 14 (2017) 332–341.
[8] X. Xi, R. Sioshansi, V. Marano, Simulation–optimization model for location of a public electric vehicle charging infrastructure, Transportation Research Part D: Transport and Environment 22 (2013) 60–69.
[9] J. Ugirumurera, Z. J. Haas, Optimal capacity sizing for completely green charging systems for electric vehicles, IEEE Transactions on Transportation Electrification 3 (2017) 565–577.
[10] X. Gan, H. Zhang, G. Hang, Z. Qin, H. Jin, Fast-charging station deployment considering elastic demand, IEEE Transactions on Transportation Electrification 6 (2020) 158–169.
[11] S. Li, F. Xie, Y. Huang, Z. Lin, C. Liu, Optimizing workplace charging facility deployment and smart charging strategies, Transportation Research Part D: Transport and Environment 87 (2020) 102481.
[12] Z. Liu, F. Wen, G. Ledwich, Optimal planning of electric-vehicle charging stations in distribution systems, IEEE transactions on power delivery 28 (2012) 102–110.
[13] L. Luo, W. Gu, S. Zhou, H. Huang, S. Gao, J. Han, et al., Optimal planning of electric vehicle charging stations comprising multi-types of charging facilities, Applied energy 226 (2018) 1087–1099.
[14] Z. J. Lee, J. Z. Pang, S. H. Low, "Pricing EV charging service with demand charge", Electric Power Systems Research 189 (2020) 106694.
[15] H. M. Ridha, C. Gomes, H. Hizam, M. Ahmadipour, A. A. Heidari, H. Chen, Multi-objective optimization and multi-criteria decision-making methods for optimal design of standalone photovoltaic system: A comprehensive review, Renewable and Sustainable Energy Reviews 135 (2021) 110202.
[16] A. Shukla, K. Verma, R. Kumar, Multi-objective synergistic planning of ev fast-charging stations in the distribution system coupled with the transportation network, IET Generation, Transmission & Distribution 13 (2019) 3421–3432.
[17] W. Yao, J. Zhao, F. Wen, Z. Dong, Y. Xue, Y. Xu, et al., A multi-objective collaborative planning strategy for integrated power distribution and electric vehicle charging systems, IEEE Transactions on Power Systems 29 (2014) 1811–1821.
[18] T. Krallmann, M. Doering, M. Stess, T. Graen, M. Nolting, Multi-objective optimization of charging infrastructure to improve suitability of commercial drivers for electric vehicles using real travel data, in: 2018 IEEE Conference on Evolving and Adaptive Intelligent Systems (EAIS), IEEE, 2018, pp. 1–8.
[19] Z. Moghaddam, I. Ahmad, D. Habibi, Q. V. Phung, Smart charging strategy for electric vehicle charging stations, IEEE Transactions on transportation electrification 4 (2017) 76–88.
[20] G. Merhy, A. Nait-Sidi-Moh, N. Moubayed, A multi-objective optimization of electric vehicles energy flows: the charging process, Annals of Operations Research 296 (2021) 315–333.
[21] R. Shi, K. Y. Lee, Multi-objective optimization of electric vehicle fast charging stations with spea-ii, IFAC-PapersOnLine 48 (2015) 535–540.
[22] H.-C. Liu, M. Yang, M. Zhou, G. Tian, An integrated multi-criteria decision making approach to location planning of electric vehicle charging stations, IEEE Transactions on Intelligent Transportation Systems 20 (2018) 362–373.
[23] S. Biswas, G. Bandyopadhyay, B. Guha, M. Bhattacharjee, An ensemble approach for portfolio selection in a multi-criteria decision making framework, Decision Making: Applications in Management and Engineering 2 (2019) 138–158.
[24] M. Žižović, B. Miljković, D. Marinković, Objective methods for determining criteria weight coefficients: A modification of the critic method, Decision Making: Applications in Management and Engineering 3 (2020) 149–161.
[25] I. Stojanović, A. Puška, Logistics performances of gulf cooperation council's countries in global supply chains, Decision Making: Applications in Management and Engineering 4 (2021) 174–193.
[26] SAE J1772, SAE Electric Vehicle and Plug in Hybrid Electric Vehicle Conductive Charge Coupler J1772, Standard, The Society of Automotive Engineers (SAE), 2012.
[27] IEC 61851-1, Electric vehicle conductive charging system- Part-I: General Requirements, Standard, International Electrotechnical Comission, 2010.
[28] F. Erden, M. C. Kisacikoglu, N. Erdogan, Adaptive V2G peak shaving and smart charging control for grid integration of PEVs, Electric Power Components and Systems 46 (2018) 1494–1508.
[29] CHAdeMO, CHAdeMO protocol and connector, 2021. URL: https://www.chademo.com/, [Online; accessed 01-May-2021].
[30] O. B. Augusto, F. Bennis, S. Caro, A new method for decision making in multi-objective optimization problems, Pesquisa Operacional 32 (2012) 331–369.
[31] A. Kesireddy, L. R. G. Carrillo, J. Baca, Multi-criteria decision making-pareto front optimization strategy for solving multi-objective problems, in: 2020 IEEE 16th International Conference on Control & Automation (ICCA), IEEE, 2020, pp. 53–58.
[32] Qingfu Zhang, Hui Li, MOEA/D: A Multiobjective Evolutionary Algorithm Based on Decomposition, IEEE Transactions on Evolutionary Computation 11 (2007) 712–731.
[33] E. C. Kara, J. S. Macdonald, D. Black, M. Bérges, G. Hug, S. Kiliccote, Estimating the benefits of electric vehicle smart charging at non-residential locations: A data-driven approach, Applied Energy 155 (2015) 515–525.
[34] M. Muratori, E. Kontou, J. Eichman, Electricity rates for electric vehicle direct current fast charging in the united states, Renewable and Sustainable Energy Reviews 113 (2019) 109235.
[35] P. Gas, E. Company, "Electric Schedule A-10, Medium General Demand-Metered Service", May 1, 2020. URL: https://www.pge.com/tariffs/index.page.
[36] M. Smith, J. Castellano, Costs associated with non-residential electric vehicle supply equipment: Factors to consider in the implementation of electric vehicle charging stations, Technical Report, U.S. Department of Energy, 2015.
[37] A. Schroeder, T. Traber, The economics of fast charging infrastructure for electric vehicles, Energy Policy 43 (2012) 136–144.

[38] C. A. C. Coello, G. B. Lamont, D. A. Van Veldhuizen, Evolutionary algorithms for solving multi-objective problems, volume 5, Springer, 2007.
[39] A. Messac, C. Puemi-Sukam, E. Melachrinoudis, Aggregate objective functions and pareto frontiers: required relationships and practical implications, Optimization and Engineering 1 (2000) 171–188.
[40] A. Malhotra, N. Erdogan, G. Binetti, I. D. Schizas, A. Davoudi, "Impact of charging interruptions in coordinated electric vehicle charging", in: 2016 IEEE Global Conference on Signal and Information Processing (GlobalSIP), IEEE, 2016, pp. 901–905.
[41] MathWorks, "Optimization Toolbox", April 30, 2020. URL: https://mathworks.com/products/optimization.html.
[42] S. Powell, E. C. Kara, R. Sevlian, G. V. Cezar, S. Kiliccote, R. Rajagopal, Controlled workplace charging of electric vehicles: The impact of rate schedules on transformer aging, Applied Energy 276 (2020) 115352.
[43] J. Dombi, A general class of fuzzy operators, the demorgan class of fuzzy operators and fuzziness measures induced by fuzzy operators, Fuzzy sets and systems 8 (1982) 149–163.
[44] C. Bonferroni, Sulle medie multiple di potenze, Bollettino dell'Unione Matematica Italiana 5 (1950) 267–270.
[45] R. R. Yager, The power average operator, IEEE Transactions on Systems, Man, and Cybernetics-Part A: Systems and Humans 31 (2001) 724–731.
[46] F. Sinani, Z. Erceg, M. Vasiljević, An evaluation of a third-party logistics provider: The application of the rough dombi-hamy mean operator, Decision Making: Applications in Management and Engineering 3 (2020) 92–107.
[47] E. K. Zavadskas, Z. Turskis, J. Antucheviciene, A. Zakarevicius, Optimization of weighted aggregated sum product assessment, Elektronika ir elektrotechnika 122 (2012) 3–6.
[48] D. Pamučar, G. Ćirović, The selection of transport and handling resources in logistics centers using multi-attributive border approximation area comparison (mabac), Expert systems with applications 42 (2015) 3016–3028.
[49] D. Pamučar, M. Mihajlović, R. Obradović, P. Atanasković, Novel approach to group multi-criteria decision making based on interval rough numbers: Hybrid dematel-anp-mairca model, Expert Systems with Applications 88 (2017) 58–80.
[50] M. Yazdani, P. Zarate, E. K. Zavadskas, Z. Turskis, A combined compromise solution (cocoso) method for multi-criteria decision-making problems, Management Decision (2019).
[51] D. Pamucar, F. Ecer, Prioritizing the weights of the evaluation criteria under fuzziness: The fuzzy full consistency method–fucom-f, Facta Universitatis, series: Mechanical Engineering 18 (2020) 419–437.
[52] S. Zolfani, M. Yazdani, D. Pamucar, P. Zarate, A VIKOR and TOPSIS focused reanalysis of the madm methods based on logarithmic normalization, arXiv preprint arXiv:2006.08150 (2020).